Intermetallics 33 (2013) 81–86

Contents lists available at SciVerse ScienceDirect

Intermetallics

journal homepage: www.elsevier.com/locate/intermet

Significant hardening due to the formation of a sigma phase matrix in a high entropy alloy

Ming-Hung Tsai [a,*], Hao Yuan [a], Guangming Cheng [a], Weizong Xu [a], Weiwei W. Jian [a], Ming-Hao Chuang [b], Chien-Chang Juan [b], An-Chou Yeh [b], Su-Jien Lin [b], Yuntian Zhu [a]

[a] Department of Materials Science and Engineering, North Carolina State University, Raleigh, NC 27695, USA
[b] Department of Materials Science and Engineering, National Tsing Hua University, Hsinchu 30013, Taiwan

ARTICLE INFO

Article history:
Received 14 July 2012
Received in revised form
23 September 2012
Accepted 25 September 2012
Available online 7 November 2012

Keywords:
B. Age-hardening
B. Precipitates
F. Electron microscopy, transmission

ABSTRACT

The hardening in $Al_{0.3}CrFe_{1.5}MnNi_{0.5}$ high-entropy alloy not only nearly triples the hardness of the alloy, but also shows a quick hardening response and the absence of overaging. However, the crystal structure, morphology, and composition of the hardening phase have not yet been confirmed. Here, such information regarding the hardening phase is investigated. It was found that the hardening phase is a Cr–Mn–Fe ternary sigma phase. Unlike in conventional engineering alloys, the sigma phase is not precipitated from the matrix, instead, the whole BCC matrix transforms to sigma phase almost without changing its composition. Therefore, the hardening phenomenon is not a precipitation hardening reaction as suggested before.

1. Introduction

High-entropy alloy (HEA) – an alloy with five or more principal elements – is a new alloy design concept proposed recently [1]. Studies show that HEAs can have high strength/hardness [1–7], outstanding wear resistance [8], exceptional high temperature strength/hardness [2,9,10], and very good structural and chemical stabilities at high temperatures [11]. Due to these properties, HEAs have great potential in many applications such as tools, molds, ring gears and other structural materials.

Most existing works on HEAs focus on the HEAs containing Al, Co, Cr, Cu, Fe, Ni, Ti elements [2–4,8,12–18]. Recently, a new HEA system with attractive properties, $Al_xCrFe_{1.5}MnNi_{0.5}$ ($x = 0.3, 0.5$), has been proposed [5]. $Al_xCrFe_{1.5}MnNi_{0.5}$ has hardness between HV 300–400 in the as-cast state. However, it can be significantly hardened when it is aged between 600 and 900 °C. For example, hardness of $Al_{0.3}CrFe_{1.5}MnNi_{0.5}$ (henceforth referred to as the $Al_{0.3}$ alloy) can be tripled from HV 299 to HV 899 when it is aged at 750 °C [19]. Although precipitation hardening was believed responsible for the significant increase in hardness, the hardening behavior is very different from that of conventional precipitation hardening. For example, the hardening response is very quick and there is no overaging. It is known that diffusion in HEAs is slower than that in conventional alloys, which is call the "sluggish diffusion effect" [20]. However, in the $Al_{0.3}$ alloy full hardening is already achieved with a short annealing time of 2 h in some cases [5]. Moreover, after achieving full hardening, the hardness remains almost at the same level up to 100 h aging. For example, hardness of the $Al_{0.3}$ alloy aged at 700 °C for 10 h and 100 h are HV 800 and HV 805, respectively [5]. The absence of overaging at such high temperature is not consistent with conventional age hardening process.

The hardening phenomenon in $Al_xCrFe_{1.5}MnNi_{0.5}$ is not understood. In particular, key information about the precipitates is lacking: the precipitates have never been observed directly, thus, the morphology and composition of the precipitates are totally unknown. Moreover, there is still no agreement among published papers on the crystal structure of the precipitates. For example, Chen et al. reported, based on XRD analysis, that the hardening phase is a $Cr_5Fe_6Mn_8$ phase [5]. However, Tsao et al., also based on XRD analysis, reported that the hardening phase belongs to σ-CrFe [19]. This is probably due to the fact that the alloy has several phases, making the XRD analysis somewhat difficult.

In this study, detailed transmission electron microscopy (TEM) analysis is performed on $Al_{0.3}CrFe_{1.5}MnNi_{0.5}$ alloy before and after the hardening process. The crystal structure, morphology, and

* Corresponding author. Department of Materials Science and Engineering, North Carolina State University, Room 300, Research Building II, 1001 Capability Dr., Raleigh, NC 27695, USA. Tel.: +1 919 515 6172; fax: +1 919 515 3419.
E-mail address: mhtsai@mx.nthu.edu.tw (M.-H. Tsai).

0966-9795/$ – see front matter © 2012 Elsevier Ltd. All rights reserved.
http://dx.doi.org/10.1016/j.intermet.2012.09.022

composition of the hardening phase are investigated, which revealed the phase transformation that led to the hardening phenomenon.

2. Experimental procedures

$Al_{0.3}CrFe_{1.5}MnNi_{0.5}$ alloy was prepared by vacuum arc melting. Raw materials with purities higher than 99.9% were melted in an Ar atmosphere for at least 3 times to ensure all of the raw materials were mixed well in their liquid state. The ingots were homogenized at 1100 °C for 4 h and then cooled in air. Some of the as-homogenized samples were then hardened at 700 °C for 2 h. Samples were ground and polished for microstructure observation in a Hitachi S3200 scanning electron microscope (SEM). Crystal structures were identified using an X-ray diffractometer (Rigaku SmartLab) in the θ–2θ configuration. A Cu Kα radiation operated at 40 kV, 44 mA was used, and the scanning speed was either 4° or 0.2° min^{-1}. Thin-foil specimens for TEM observation were prepared by mechanical thinning followed by ion milling. The foils were then observed on a 200 keV TEM (JOEL JEM-2010F) with energy dispersive X-ray spectroscopy (EDS) capability. Macro-hardness (the "overall" hardness in Table 1) and micro-hardness were measured using hardness testers (Mitutoyo HV-115 and HM-115) under loads of 5 kg and 25 g, respectively. Micro-hardness indentation was conducted in the dendritic and the inter-dendritic regions. Size of the indented area was 5–10 μm and that of the characteristic features is 3–8 times larger.

3. Results and discussion

Fig. 1(a) shows the XRD patterns of as-homogenized and annealed alloys. As-homogenized alloy is composed of a major BCC phase and a minor FCC phase, which is in agreement with previous reports [5,19]. After annealing, the intensity of BCC peaks decreased significantly. Another set of peak, which corresponds to the age-hardening phase, appears. The intensity of FCC peaks remains roughly unchanged. This suggests that the age-hardening phase is converted from the BCC phase. To obtain an XRD pattern of the hardening phase that has high signal-to-noise ratio, a slow scan speed of 0.2° min^{-1} was used. Fig. 1(b) shows an example section of such pattern. It can be seen that the signal-to-noise ratio is good enough to clearly identify all the peaks. From the pattern, the structure of the age-hardening phase is indexed to be same as σ-CrFe (JCPDS no. 005-0708), which means it has a tetragonal structure (space group: P42/mnm). The lattice constants are: $a = 8.8090$ Å and $c = 4.5519$ Å. The hardening phase will henceforth be referred to as the sigma phase.

The microstructure of the annealed alloy retained the cast dendrite–interdendrite structure [Fig. 2(a)]. From previous literature [5], in the as-cast alloy the dendrite region has a BCC structure and the interdendrite has an FCC structure. Since the XRD patterns suggest that the sigma phase is converted from the BCC phase, the sigma phase would be expected to reside in the dendrite region. Indeed, microhardness measurements (Table 1) taken in the dendrite and interdendrite regions reveal that the dendrite is hardened from HV 386 to HV 1045, while the interdendrite was not

Table 1
Hardness of the dendrite and interdendrite regions in the $Al_{0.3}CrFe_{1.5}MnNi_{0.5}$ alloy before and after the hardening heat treatment.

	Hardness (HV)		
	Overall	Dendrite	Interdendrite
As-homogenized	317 ± 9	386 ± 5	261 ± 15
Annealed (700 °C, 2 h)	840 ± 23	1045 ± 30	258 ± 29

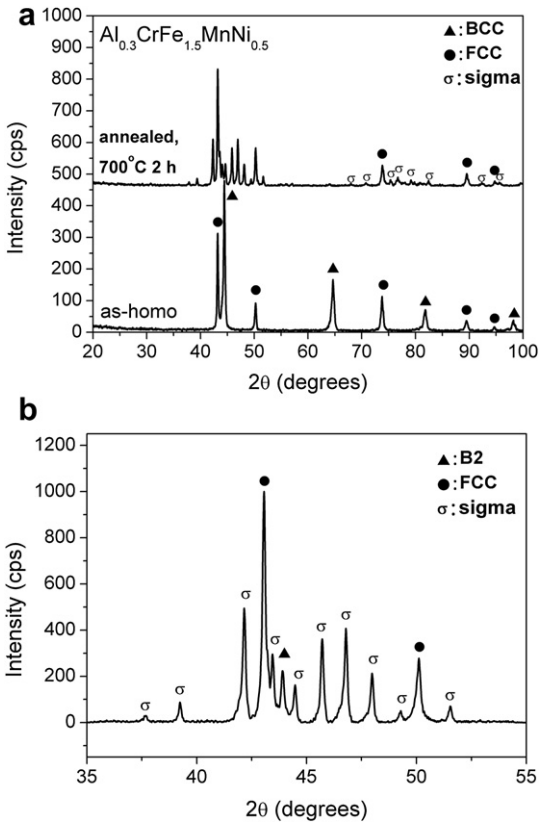

Fig. 1. (a) The XRD patterns of the as-homogenized alloy and the annealed alloy. (b) An example section of the XRD pattern of the annealed alloy obtained using a slow scan speed of 0.2° min^{-1}.

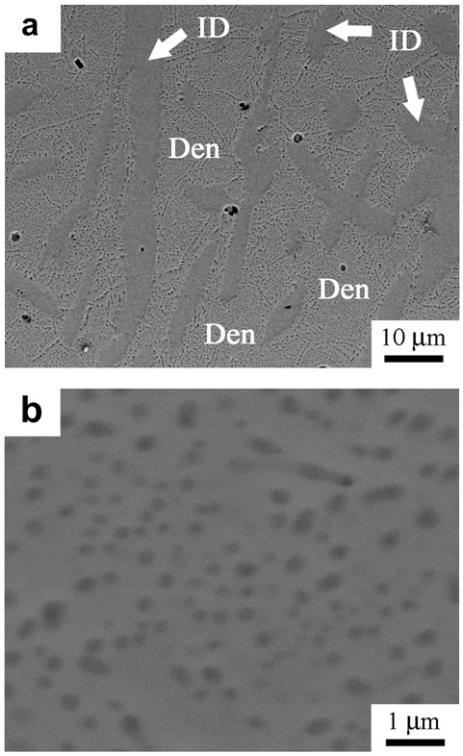

Fig. 2. (a) SEM images of the annealed alloy. (b) High-magnification image of the dendrite region in (a).